Annealing temperature effect on structural, vibrational and optical properties of $Co_{0.8}Ni_{0.2}Fe_2O_4$ nanoparticles

J Utomo[1], A K Agustina[1] and E Suharyadi[1*]

[1] Department of Physics, Gadjah Mada University, North Sekip BLS Yogyakarta 55281, Indonesia

*esuharyadi@ugm.ac.id

Abstract. $Co_{0.8}Ni_{0.2}Fe_2O_4$ nanoparticles were synthesized by coprecipitation method and annealed at different temperatures (200, 400, 600, 800 and 1000 °C). The X-ray diffraction (XRD) exhibited the formation of spinel cubic structure. The crystallite size of $Co_{0.8}Ni_{0.2}Fe_2O_4$ nanoparticles at the annealing temperature of 200 °C was 7.0 nm and then increased with the increase of annealing temperature. The reason for this is that the particles grow faster and larger at a higher temperature. The transmission electron microscopy (TEM) images showed that the size distribution of the particles was increased with the increase of annealing temperature. It was also seen from the samples that most of the particles appeared nearly spherical in shape with slight agglomeration, particularly at higher annealing temperature. The Fourier transform infrared spectroscopy (FTIR) spectra of $Co_{0.8}Ni_{0.2}Fe_2O_4$ nanoparticles confirmed the presence of vibration bands of metal ions at 370.30 – 401.9 cm^{-1} and 586.36 – 601.79 cm^{-1} which was in a region of octahedral and tetrahedral sites, respectively. The values of the gap energy of $Co_{0.8}Ni_{0.2}Fe_2O_4$ nanoparticles observed ultraviolet-visible (UV-Vis) spectroscopy were in the range of 4.25 – 4.94 eV. The gap energy was decreased with the increase of annealing temperature and the increase of crystallite size.

1. Introduction

Spinel ferrite nanoparticles having the general chemical formula MFe_2O_4 (M is divalent metal cation) are attractive materials because of their applications in such fields as drug delivery, spintronics, high-density information storage, microwave devices, and optoelectronics [1-3]. They have excellent chemical and physical properties which could not be found in the bulk size due to their large surface area [4]. Among spinel ferrite nanoparticles, recently Co-Ni ferrite are most fascinating materials to be investigated. Cobalt ferrite and nickel ferrite have inverse spinel structure with all of the Co^{2+}/Ni^{2+} ions occupied at octahedral (B) site and Fe^{3+} ions distributed between tetrahedral (A) and octahedral (B) sites [5]. In addition, cobalt ferrite is hard magnetic materials with high chemical stability and mechanical hardness while nickel ferrite is soft magnetic materials with high resistivity more than 10^9 Ωcm [6, 7]. Therefore Co-Ni ferrite is suitable to be applied for high-frequency electronic devices e.g. isolators and circulators due to their high electrical resistivity and good magnetic properties [8, 9].
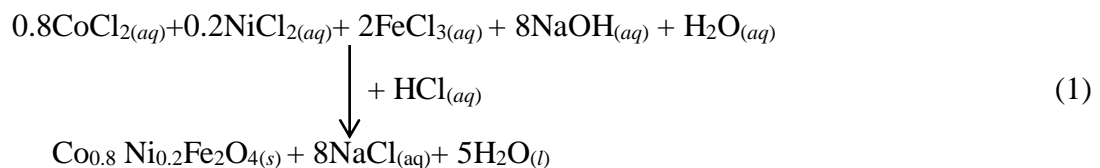
To achieve these applications, it is necessary to consider the quality of crystal through their properties. Their properties are mainly affected by particles size, shape, crystallinity and cation distribution between tetrahedral (A) and octahedral (B) sites [10, 11]. One of the main factors that determine the quality of crystal is the preparation method. It is important to consider obtaining well ferrite performance and also preparing easily. Coprecipitation method is one of the methods chosen by

many researchers because this method is simpler, low cost and used low synthesis temperature. Another reason is that this method could control the production of ferrite particles [12]. However, this method produces tiny particle size causing agglomeration. It mainly affects the weakening of their properties such as structural, vibrational and optical properties. Therefore, the weakening of their properties could be handled by giving annealing temperature after synthesis process [13]. Their properties of spinel ferrite could be improved by the effect of annealing temperature to reach well crystallinity and reduce agglomeration. The objective of this investigation is to explore structural, vibrational and optical properties of $Co_{0.8}Ni_{0.2}Fe_2O_4$ nanoparticles annealed at various annealing temperatures and synthesized by coprecipitation method. Correlation between annealing temperature on structural, vibrational and optical properties will be carried out in detail.

2. Experimental method

$Co_{0.8}Ni_{0.2}Fe_2O_4$ nanoparticles were synthesized by coprecipitation method. Cobalt chloride hexahydrate $(CoCl_2.6H_2O)$, nickel chloride hexahydrate $(NiCl_2.6H_2O)$ and iron chloride hexahydrate $(FeCl_3.6H_2O)$ were used as precursors by dissolving them in distilled water with the concentration of 0.16 M, 0.04 M and 0.4 M, respectively. The mixture was added to HCl as a catalyst. And then, the mixture solution was added drop wise to the NaOH solution (12 M) heated at a synthesis temperature of 90 °C while homogenized at constant stirring (1000 rpm) for 1 hour. The chemical reaction of $Co_{0.8}Ni_{0.2}Fe_2O_4$ nanoparticles could be described as:

$$0.8CoCl_{2(aq)}+0.2NiCl_{2(aq)}+ 2FeCl_{3(aq)} + 8NaOH_{(aq)} + H_2O_{(aq)}$$
$$+ HCl_{(aq)} \qquad (1)$$
$$Co_{0.8}Ni_{0.2}Fe_2O_{4(s)} + 8NaCl_{(aq)}+ 5H_2O_{(l)}$$

The prepared precipitate was then rinsed five times with distilled water until the rinsing was free from the traces of sodium, chloride and other impurities. The precipitate was subsequently dried at 90 °C in a furnace for 4 hours to remove traces of water. Afterward, the resulting powder was annealed at different temperatures (200, 400, 600, 800 and 1000 °C). The structural properties and morphologies of $Co_{0.8}Ni_{0.2}Fe_2O_4$ nanoparticles at different annealing temperatures were studied by X-ray diffractometer (XRD) using Cu-K_α radiation with wavelength λ=1.5406 Å and transmission electron microscope (TEM) Jeol JEM-1400. The vibrational spectra were recorded by Fourier transform infrared spectroscope (FTIR) Prestige Shimadzu-21 at room temperature. The optical properties of samples were analyzed by UV-Vis spectrophotometer DR 1700 PharmaSpec.

3. Results and discussion

3.1. X-Ray diffraction analysis

Figure 1 shows the XRD patterns of $Co_{0.8}Ni_{0.2}Fe_2O_4$ nanoparticles for as-prepared and annealed at 200, 400, 600, 800 and 1000 °C. There are reflection planes for all samples such as (220), (311), (400), (422), (511) and (440) indicating the formation of cubic spinel structure with space group *Fd3m* (JCPDS card no #22-1086) [14]. $Co_{0.8}Ni_{0.2}Fe_2O_4$ nanoparticles have nearly single phase without any new phases detected. The increase of annealing temperature results in an enhancement of crystallinity degree where the peak intensity (311) increases while the full width at the half maximum (FWHM) decreases for $Co_{0.8}Ni_{0.2}Fe_2O_4$ nanoparticles. The structural parameters such as lattice parameter, crystallite size, microstrain and X-ray density could be obtained from the XRD data. The lattice parameter *a* is calculated according to the Bragg's formula [7]. The crystallite size *D* is estimated according to the Scherrer's formula [15].
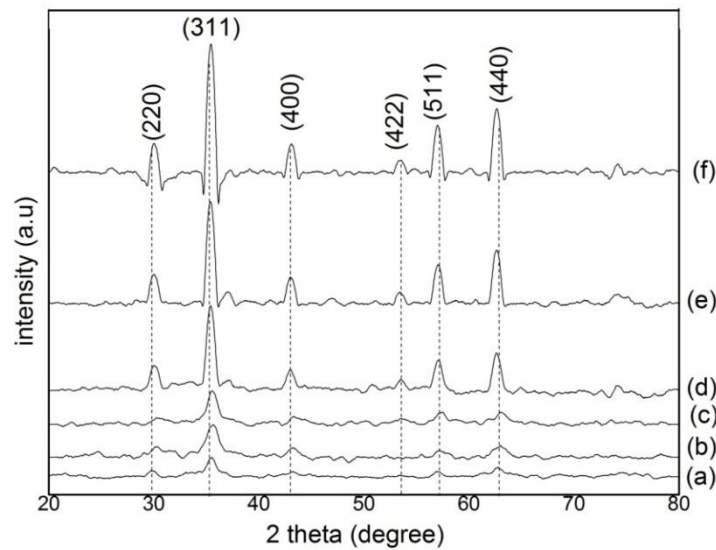
Figure 1. XRD patterns of $Co_{0.8}Ni_{0.2}Fe_2O_4$ nanoparticles at different annealing temperatures (a) as-prepared (AP), (b) 200 °C, (c) 400 °C, (d) 600 °C, (e) 800 °C and (f) 1000 °C.

The structural parameters from the XRD patterns of $Co_{0.8}Ni_{0.2}Fe_2O_4$ nanoparticles for as-prepared and annealed samples are shown in Table 1. The data obtained from XRD analysis reveals an increasing pattern in crystallite size with the increase of annealing temperature as shown in Table 1. This is due to the crystallite size at higher annealing temperature enhances the coalescence process of crystallites into a larger average size of nanoparticles [4].

Table 1. Lattice parameter, crystallite size, X-ray density and strain of $Co_{0.8}Ni_{0.2}Fe_2O_4$ nanoparticles.

| Anealling temperature (°C)	Lattice parameter (Å)	Crystallite size (nm)	X-ray density (g/cm³)	Microstrain ($\times 10^2$ /line²)
AP	8.38	10.4	5.3	4.4
200	8.35	7.0	5.3	6.5
400	8.36	8.3	5.3	5.5
600	8.39	9.6	5.2	4.7
800	8.40	9.8	5.2	4.6
1000	8.39	10.5	5.2	4.3

The lattice parameter has an increasing trend with the increase of annealing temperature which is in the range 8.35 Å – 8.40 Å. This is attributed to faster coarsening process when a higher annealing temperature is applied to the samples. A faster coarsening process causes enhancement in unit cell volume which results in increasing lattice parameter. The X-ray density decreases with the increase of annealing temperature. This is caused by the increase of annealing temperature results in larger unit cell volume of nanoparticles as shown in the following formula [16].

$$\rho_x = \frac{8M}{NV} \tag{2}$$

where ρ_x is X-ray density, V is unit cell volume, N is the Avogadro's number and M is molecular weight of $Co_{0.8}Ni_{0.2}Fe_2O_4$ nanoparticles.

3.2. Transmission electron microscopic (TEM) images

Figure 2 shows the morphology of $Co_{0.8}Ni_{0.2}Fe_2O_4$ nanoparticles for as-prepared and annealed at 400, 600, 800 and 1000 °C. The particles are initially agglomerated in a spherical shape at an annealing temperature of 400 °C. Subsequently, the particles are nearly in cubic shape with slight agglomeration at annealing temperatures of 600 and 800 °C. And then, the particles are agglomerated at an annealing temperature of 1000 °C. From TEM images, it is confirmed that the particles size increases with the increase of annealing temperature. This result supports XRD analysis that has been studied previously. This phenomenon is caused the particles grow faster and form larger at higher annealing temperature [17]. The selected area electron diffraction (SAED) patterns of the $Co_{0.8}Ni_{0.2}Fe_2O_4$ nanoparticles for as-prepared, annealed at 400 °C and 600 °C display continuous polycrystalline rings while for samples annealed at 800 and 1000 °C display discontinuous polycrystalline. All of the samples reveal polycrystalline nature.
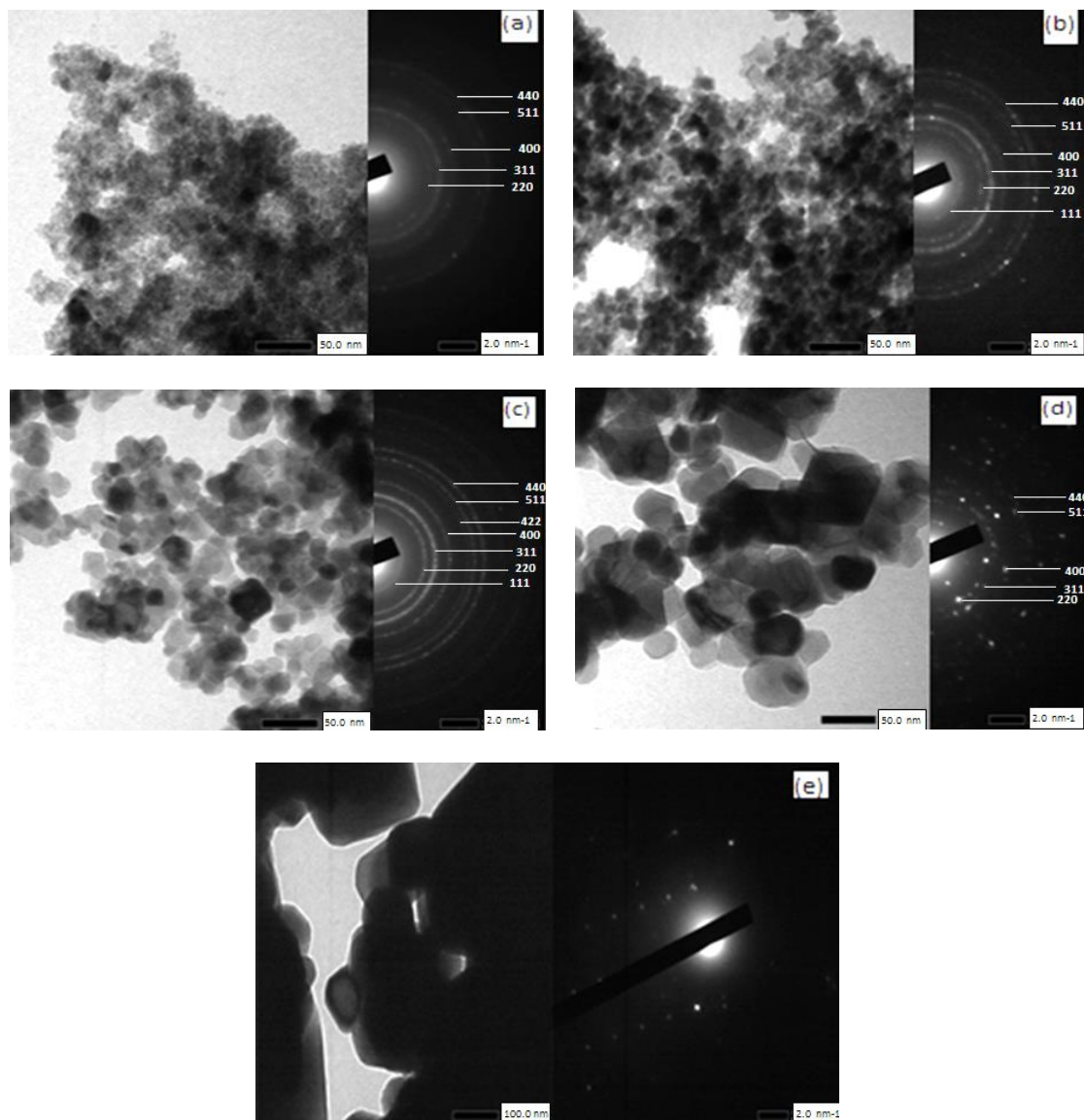
Figure 2. TEM images of of $Co_{0.8}Ni_{0.2}Fe_2O_4$ nanoparticles at different annealing temperatures (a) as-prepared (AP), (b) 400 °C, (c) 600 °C, (d) 800 °C and (e) 1000 °C.

3.3. Fourier transform infrared spectroscopy (FTIR) studies

The vibrational spectra of $Co_{0.8}Ni_{0.2}Fe_2O_4$ nanoparticles for as-prepared and annealed were observed by FTIR spectroscope at room temperature as shown in Figure 4. According to the Figure 3, there are two metal oxygen (M – O) bands which are in wave number 370.3 cm^{-1} – 401.19 cm^{-1} and 586.36 cm^{-1} – 601.79 cm^{-1}. They are respectively at octahedral and tetrahedral sites indicating the formation of spinel ferrite structure.
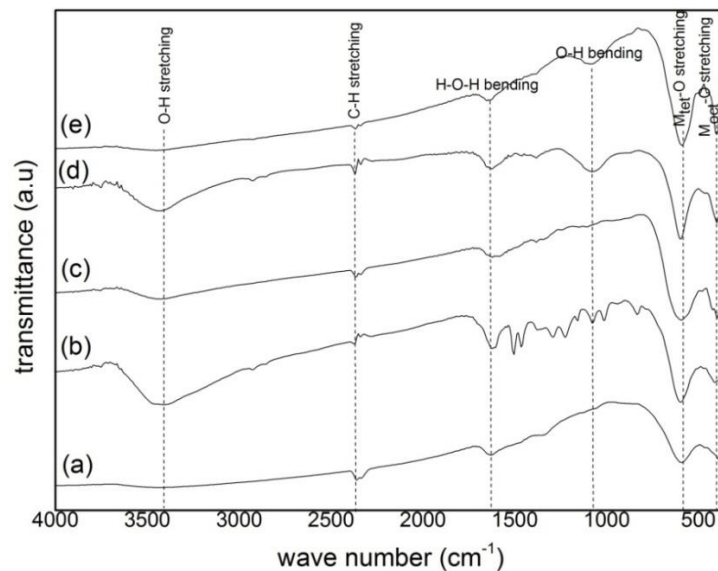
Figure 3. Vibrational spectra of $Co_{0.8}Ni_{0.2}Fe_2O_4$ nanoparticles at different annealing temperatures (a) as-prepared, (b) 400 °C, (c) 600 °C, (d) 800 °C and (e) 1000 °C.

The detailed wave number of M – O at octahedral and tetrahedral sites are shown in Table 2. From Table 2, the wave number of M – O stretching vibration at the octahedral site is lower than the tetrahedral site. This could be attributed to shorter or longer bond length of the octahedral or tetrahedral site. In addition, the wave number of octahedral sites is shifted toward higher wave number with the increase of annealing temperature. This is related to their atomic weight of ions. The absorption band at 3410 – 3448.72 cm^{-1} is attributed to the hydroxyl (O – H) group of stretching vibration. This is also observed that the intensity of this absorption band has a decreasing trend with the increase of annealing temperature. This may be attributed to the loss the residual water in the nanoparticles [18]. The appeared absorption band at 1581 – 1651.7 cm^{-1} for all samples correspond to the existence of H_2O molecules [7, 10].

Table 2. The wave number of metal-oxygen vibration at octahedral and tetrahedral sites of as-prepared and annealed $Co_{0.8}Ni_{0.2}Fe_2O_4$ nanoparticles.

Anealling temperature (°C)	Wave number (cm^{-1})	
	Octahedral site	Tetrahedral site
AP	370.3	594.08
400	385.76	594.08
600	401.19	594.08
800	401.19	601.79
1000	401.19	586.36

3.4. UV-Vis analysis

The optical gap energy of $Co_{0.8}Ni_{0.2}Fe_2O_4$ nanoparticles for as-prepared and annealed was carried out by using UV-visible spectroscope. Figure 4 shows the dependence of the optical gap energy on annealing temperature. According to the Figure 4, the optical gap energy decreases with the increase of annealing temperature.
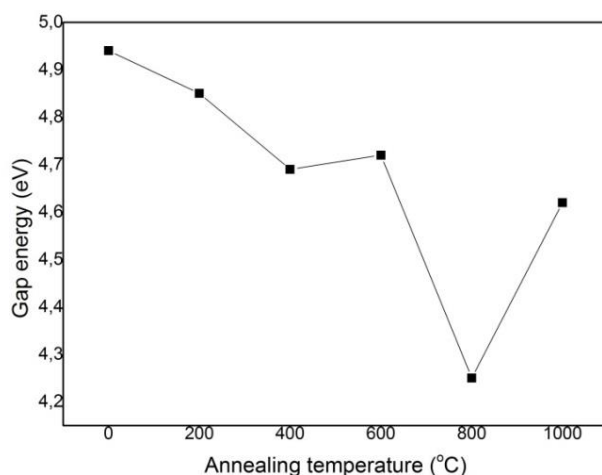
Figure 4. The dependence of the optical gap energy
on annealing temperature.

The decrease of gap energy may be attributed to the Burstein-Moss Effect. Also, the reduction of gap energy shows that the photon absorption is shifted toward higher wave length (red shift). This shift could be caused by the strong interaction (s-d and p-d) result into a positive and negative correction to the valence and conduction band edges [19]. In addition, there is a correlation between crystallite size and optical gap energy as shown in Table 3.The optical band energy decrease with the increase of crystallite size. This is related to an enhancement of crystallinity when the higher annealing temperature is applied [4].

Table 3. Gap energy of as-prepared and annealed $Co_{0.8}Ni_{0.2}Fe_2O_4$ nanoparticles.

Anealling temperature (°C)	Crystallite size (nm)	Gap energy (eV)
AP	10.4	4.94
200	7.0	4.85
400	8.3	4.69
600	9.6	4.72
800	9.8	4.25
1000	10.5	4.62

4. Conclusion

We have synthesized $Co_{0.8}Ni_{0.2}Fe_2O_4$ nanoparticles using coprecipitation method and then annealed them at various temperatures. The XRD analysis reveals that $Co_{0.8}Ni_{0.2}Fe_2O_4$ nanoparticles for as-prepared and annealed have the formation of the cubic spinel structure. The crystallite size and lattice parameter display an increasing trend while the X-ray density and microstrain shows a decreasing trend

with the increase of annealing temperature. TEM images and FTIR spectra confirm the formation of the cubic spinel structure. The annealing temperature decreases the value of the optical gap energy.

References

[1]   Singhal S Singh J Barthwal S K and Chandra K 2005 *J. Solid State Chem* **178** 3183-9

[2]   Kumar A Sharma P and Varshney D 2014 *Ceram. Int* **40** 12855-60

[3]   Jiang J 2007 *Mater. Lett* **61** 3239-42

[4]   Othman A A Osman M A Ibrahim E M M and Ali M A 2015 *Ceram. Int* **43** 527-33

[5]   Mathew D S and Juang R 2007 *Chem. Eng. J* **129** 51-65

[6]   Kambale R C Shaikh P A Kambale S S and Kolekar Y D 2009 *J. Alloys Compd* **478** 599-603

[7]   Kumar A K Yadav N Rana D S Kumar P Arora M and Pant R P 2015 *J. Magn. Magn. Mater* **394** 379-84

[8]   Kafeni K K Msagati T A M and Mamba B B 2017 *Mater. Sci.. Eng B* **215** 37-55

[9]   Xiang J Chu Y Shen X Zhou G and Guo Y 2012 *J. Colloid and Interface Sci.* **376** 57-61

[10] Awati V V Rathod S M Mane M L and Mohite K C 2013 *Int. Nano. Lett* **3** 29

[11] Saffari F Kameli P Rahimi M Ahmadvand H and Salamati H 2015 *Ceram. Int* **41** 7352-8

[12] Maaz K Karim S and Kim G 2012 *Chem. Phys. Lett* **549** 67-71

[13] Indrayana I P T Siregar N Suharyadi E Kato T and Iwata S 2016 *J. Phys: Conf. Series* **776** 012021

[14] Kasapoglu N Birsöz B Baykal A Köseoglu Y and Toprak M S 2007 *Cent. Eur. J. Chem* **5** 570-80

[15] Pugazhvadivu K S Ramachandran K and Tamilarasan K 2013 *Phys. Proc* **49** 205-16

[16] Sontu U B Yelasani V and Musugu V R R 2015 *J. Magn. Magn. Mater* **374** 376-80

[17] Abdallah H M I Moyo T and Ngema N 2015 *J. Magn. Magn. Mater* **394** 223-8

[18] Azhagushanmugam S J Suriyanarayanan N and Jayaprakash R 2013 *Phys. Proc* **49** 44-8

[19] Sharma D and Jha R 2017 *J. Alloys Compd* **698** 532-8